Electronic Supplementary Material (ESI) for Faraday Discussions.

SUPPORTING INFORMATION

A High-Throughput Screening of Metal-Organic Framework Based Membranes for Biogas Upgrading

Joseph Glover [†] ***and Elena Besley****

School of Chemistry, University of Nottingham, Nottingham, NG7 2RD (UK)

† Current Address: School of Chemistry, University of Southampton, Highfield, Southampton, SO17 3QZ (UK)

*Corresponding author: E-mail: Elena.Besley@nottingham.ac.uk

1. Force-field parameters, geometric criteria, and experimental conditions

Table S1. *List of UFF force-field[1] parameters and oxidation states (O.S) used for EQeq calculations in this work.*

Element	O.S	ε (K)	σ (Å)	Element	O.S	ε (K)	σ (Å)	Element	O.S	ε (K)	σ (Å)	Element	O.S	ε (K)	σ (Å)
Ac	+3	16.6	3.10	Er	+1	3.52	3.02	N	0	34.72	3.26	Si	+4	202.27	3.83
Ag	+1	18.11	2.80	Es	+3	6.04	2.94	Na	+1	15.09	2.66	Sm	+1	3.1359	3.14
Al	+3	254.09	4.01	Eu	+1	4.03	3.11	Nb	+4	29.69	2.82	Sn	+2	285.28	3.91
Am	+3	7.04	3.01	F	0	25.16	3.00	Nd	+1	5.03	3.18	Sr	+2	118.24	3.24
Ar	0	93.08	3.45	Fe	+2	6.54	2.59	Ne	0	21.13	2.66	Ta	0	40.75	2.82
As	+3	155.47	3.77	Ga	+3	208.81	3.90	Ni	+2	7.55	2.52	Tb	+1	3.52	3.07
At	0	142.89	4.23	Gd	+1	4.53	3.00	Np	+4	9.56	3.05	Tc	+2	24.154	2.671
Au	+1	19.62	2.93	Ge	+2	190.69	3.81	O	0	30.19	3.12	Te	0	200.25	3.98
B	0	90.57	3.64	H	0	22.14	2.57	Os	0	18.62	2.78	Th	+4	13.08	3.03
Ba	+2	183.15	3.30	He	0	10.9	2.64	P	0	153.46	3.69	Ti	+4	8.55	2.83
Be	+2	42.77	2.45	Hf	+3	36.23	2.8	Pb	+2	333.59	3.83	Tl	+1	342.14	3.87
Bi	+3	260.63	3.89	Hg	+1	193.71	2.41	Pd	+2	24.15	2.58	Tm	+2	3.02	3.006
Br	0	126.29	3.73	Ho	+1	3.52	3.04	Pm	+1	4.53	3.16	U	+3	11.07	3.02
C	0	52.83	3.43	I	0	170.57	4.01	Pr	+3	5.03	3.21	V	+4	8.05	2.8
Ca	+2	119.75	3.03	In	+3	301.39	3.98	Pt	+1	40.25	2.45	W	0	33.71	2.73
Cd	+2	114.72	2.54	Ir	0	36.73	2.53	Pu	+4	8.05	3.05	Xe	0	167.04	3.92
Ce	+3	6.54	3.17	K	+1	17.61	3.40	Rb	+1	20.13	3.67	Y	+3	36.23	2.98
Cl	0	114.21	3.52	Kr	0	110.69	3.69	Re	0	33.21	2.63	Yb	+2	114.72	2.99
Cm	+3	6.54	2.96	La	+2	8.55	3.14	Rh	+2	26.67	2.61	Zn	+2	62.39	2.46
Co	+2	7.04	2.56	Li	+1	12.58	2.18	Ru	+2	28.18	2.64	Zr	+4	34.72	2.78
Cr	+3	7.55	2.69	Lu	+1	20.63	3.24	S	0	137.86	3.59				
Cs	+1	22.64	4.02	Mg	+2	55.85	2.69	Sb	+3	225.91	3.94				
Cu	+2	2.52	3.11	Mn	+2	6.54	2.64	Sc	+3	9.56	2.94				
Dy	+1	3.52	3.05	Mo	+4	28.18	2.72	Se	0	146.42	3.75				

Table S2. *List of force-field parameters for adsorbates models taken directly from our RASPA inputs.*

Molecule	Atom	σ (Å)	ε (K)	q	Reference
CH_4	CH_4	3.73	148	0.000	[2]
CO_2	C	2.80	27.0	+0.700	[3]
	O	3.05	79.0	-0.350	
H_2S	H	0.00	0.00	+0.250	[4]
	S	3.73	250	+0.400	
	M	0.00	0.00	-0.900	
H_2O	H	0.00	0.00	+0.52422	[5]
	O	3.16435	81.8994972	0.000	
	M	0.00	0.00	-1.04844	

Models

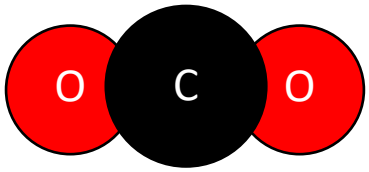

r_{C-O} = 1.16 Å

$<_{OCO}$ = 180°

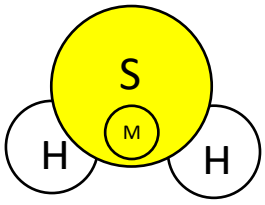

r_{S-H} = 1.34 Å

r_{S-M} = 0.186 Å

$<_{HSH}$ = 92.0°

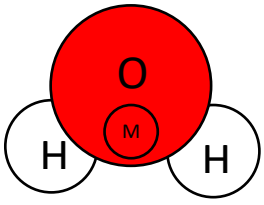

r_{O-H} = 0.9572 Å

r_{O-M} = 0.125 Å

$<_{HOH}$ = 104.52°

Table S3. *List of experimental conditions used in comparison calculations*

MOF	Membrane Thickness (μm)	Gases	Temp (K)	Pressure (bar)	Reference
IRMOF-1	25	CO_2, CH_4	298	1.06	[6]
Ni-MOF-74	25	CO_2, CH_4	298	1.80	[7]
ZIF-8	5	50:50 CO_2/CH_4 mixture	298	1.00	[8]
ZIF-90	20	CO_2, CH_4	473	1.00	[9]
Bio-MOF-1	15	50:50 CO_2/CH_4 mixture	298	1.00	[10]

Geometric Criteria

Geometric properties such as accessible surface area (ASA), pore limiting diameter (PLD), largest cavity diameter (LCD), pore volume (PV), void fraction (φ) and density were calculated using Zeo++ version 0.3.[11] ASAs were calculated using a 1.86 Å radius probe and 5000 monte-carlo (MC) insertions per atom, while PVs were calculated using a 0 Å radius probe and 50,000 insertions per unit cell. PLDs and LCDs were calculated from the largest spheres that did not overlap with any framework atoms. Only frameworks that possessed non-zero ASAs were considered in this study. Furthermore, we excluded frameworks with PLDs < 3.80 Å which would not permit the diffusion of each main biogas component, (i.e. Kinetic diameters: CH_4 (3.80 Å), CO_2, (3.30 Å) or H_2S (3.60 Å)).

2. Partial charge analysis of ligands

In recent work, Ongari and co-workers compared the charges obtained from different QEq variants against DDEC charges for 2338 MOFs.[12] Using data from DDEC charge distributions, they showed that by imposing an upper and lower atomic charge limit of +3 and -2 respectively, fewer structures containing un-physical charges were obtained from using the higher oxidation state Taylor expansion. While this charge criteria worked well for identifying metals with unphysical charges, it failed to identify some ligand atoms that possess unphysical or unrealistic charges (e.g. C charge between +2 and +3). This is shown in the following histograms where we examined the atomic partial charge distributions of the 7109 MOFs from the end of Phase 1 calculations.

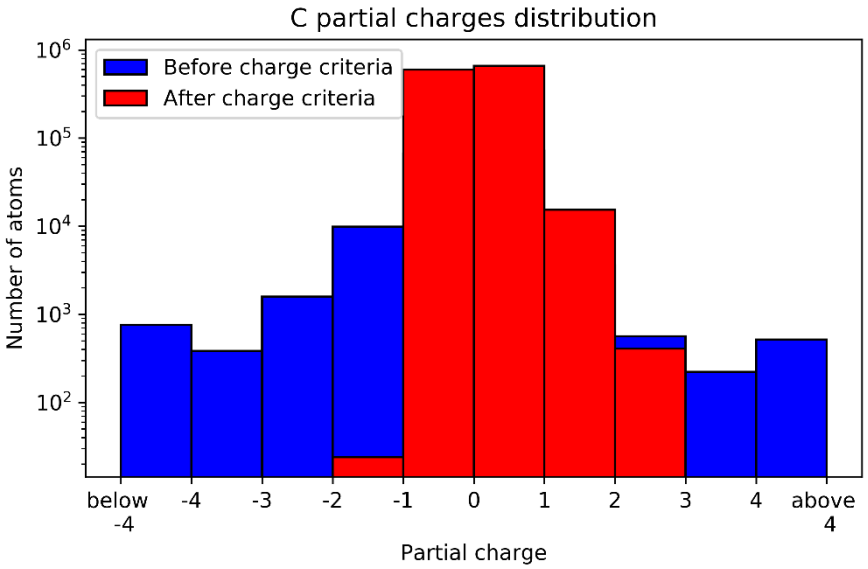

Figure S1. *Partial charge distribution of all carbon atoms in our initial 7109 MOFs compared before and after applying Ongari et al's charge criteria.*

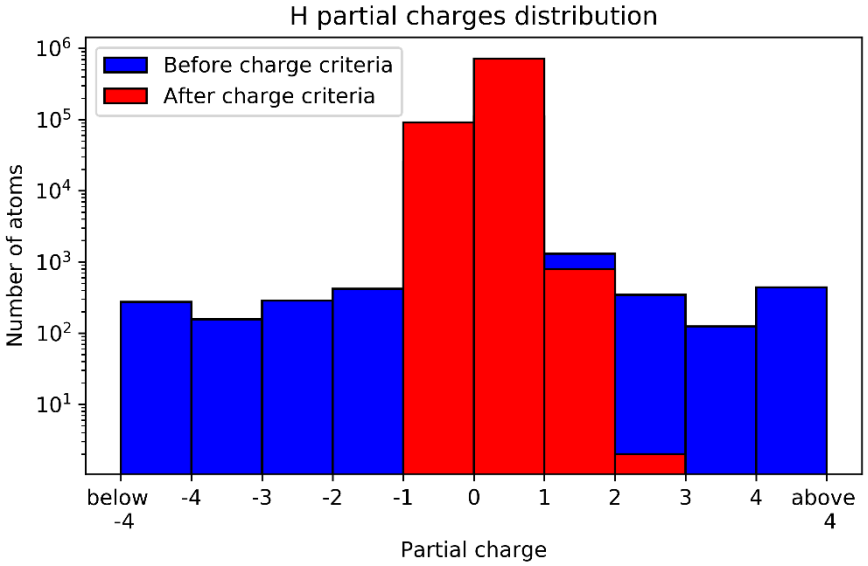

Figure S2. *Partial charge distribution of all hydrogen atoms in our initial 7109 MOFs compared before and after applying Ongari et al's charge criteria.*

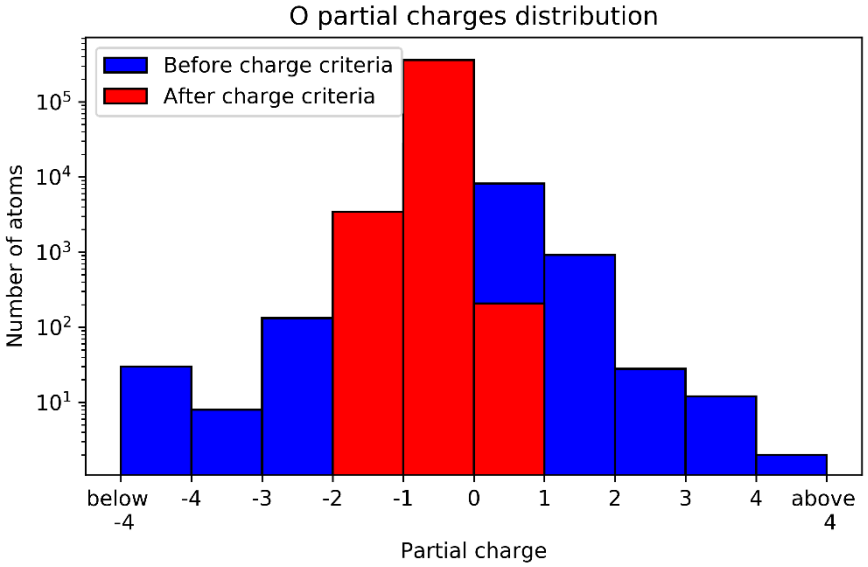

Figure S3. *Partial charge distribution of all oxygen atoms in our initial 7109 MOFs compared before and after applying Ongari et al's charge criteria.*

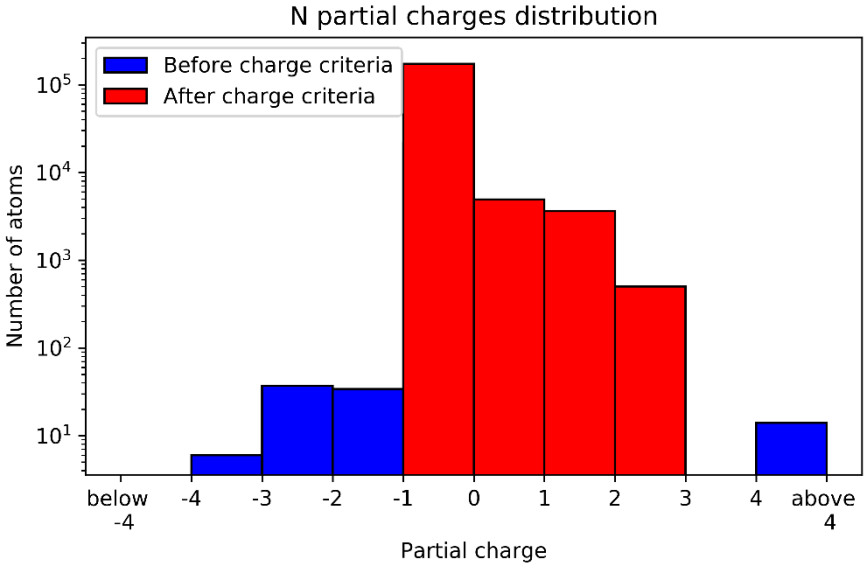

Figure S4. *Partial charge distribution of all nitrogen atoms in our initial 7109 MOFs compared before and after applying Ongari et al's charge criteria.*

3. Heat of adsorption distributions at infinite dilution

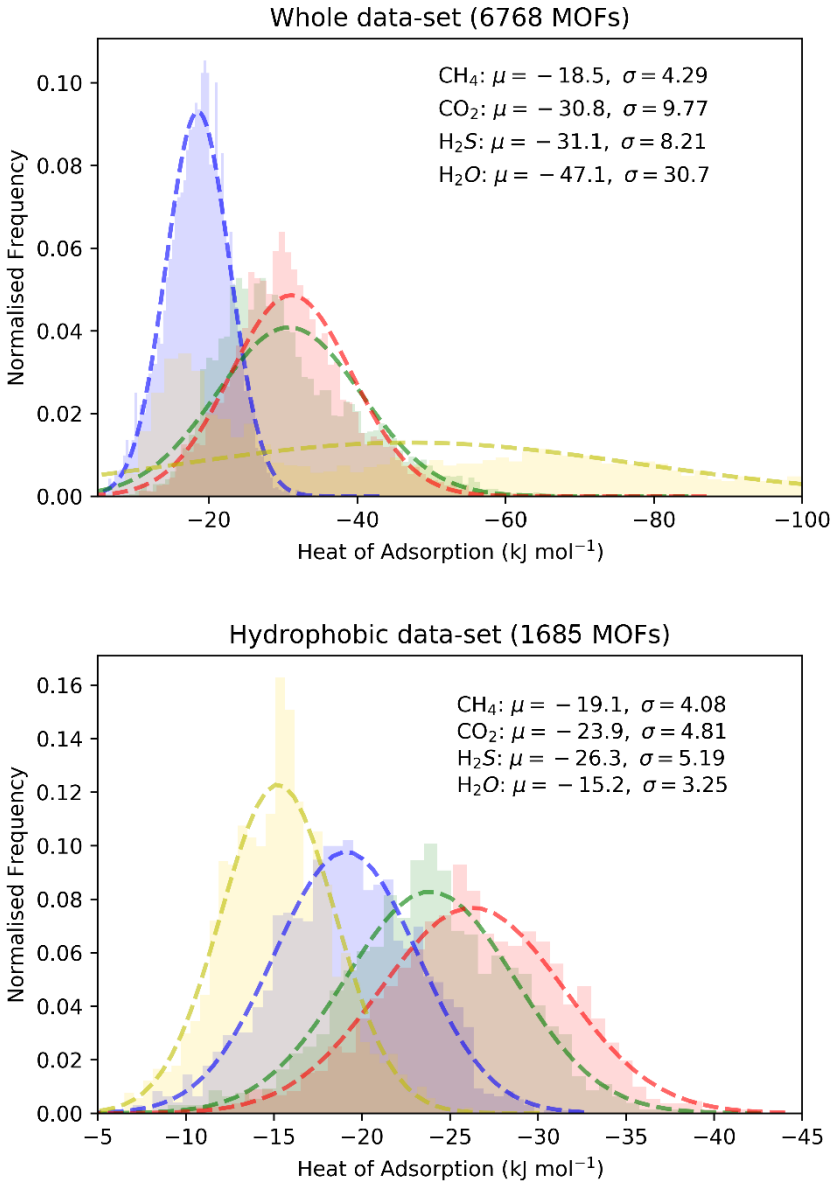

Figure S5. *Comparison of the heat of adsorption distributions in the 6768 MOFs from the 2nd phase of calculations and the 1685 hydrophobic MOFs. Colour scheme: Red = H_2S, Green = CO_2, Blue = CH_4, Yellow = H_2O*

4. Impact of hydrophobicity criteria

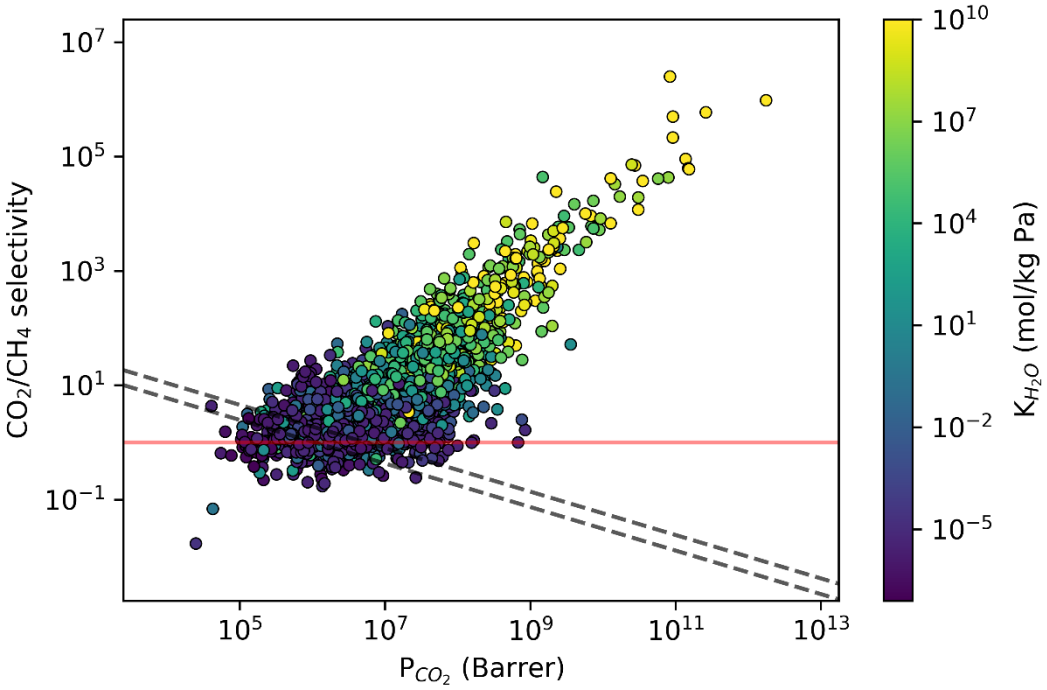

Figure S6. *Robeson plot for all 6768 MOFs studied in this work (those with converged EQeq calculations). Each point is a separate structure that is coloured with respect to the H_2O Henry coefficient in that structure.*

5. Void analysis images of top eight MOFs

Voids were determined using a probe size of 1.2 Å and a grid spacing of 0.7 Å using the Mercury software package.[13] The pores of each structure are shown along the channel axis.

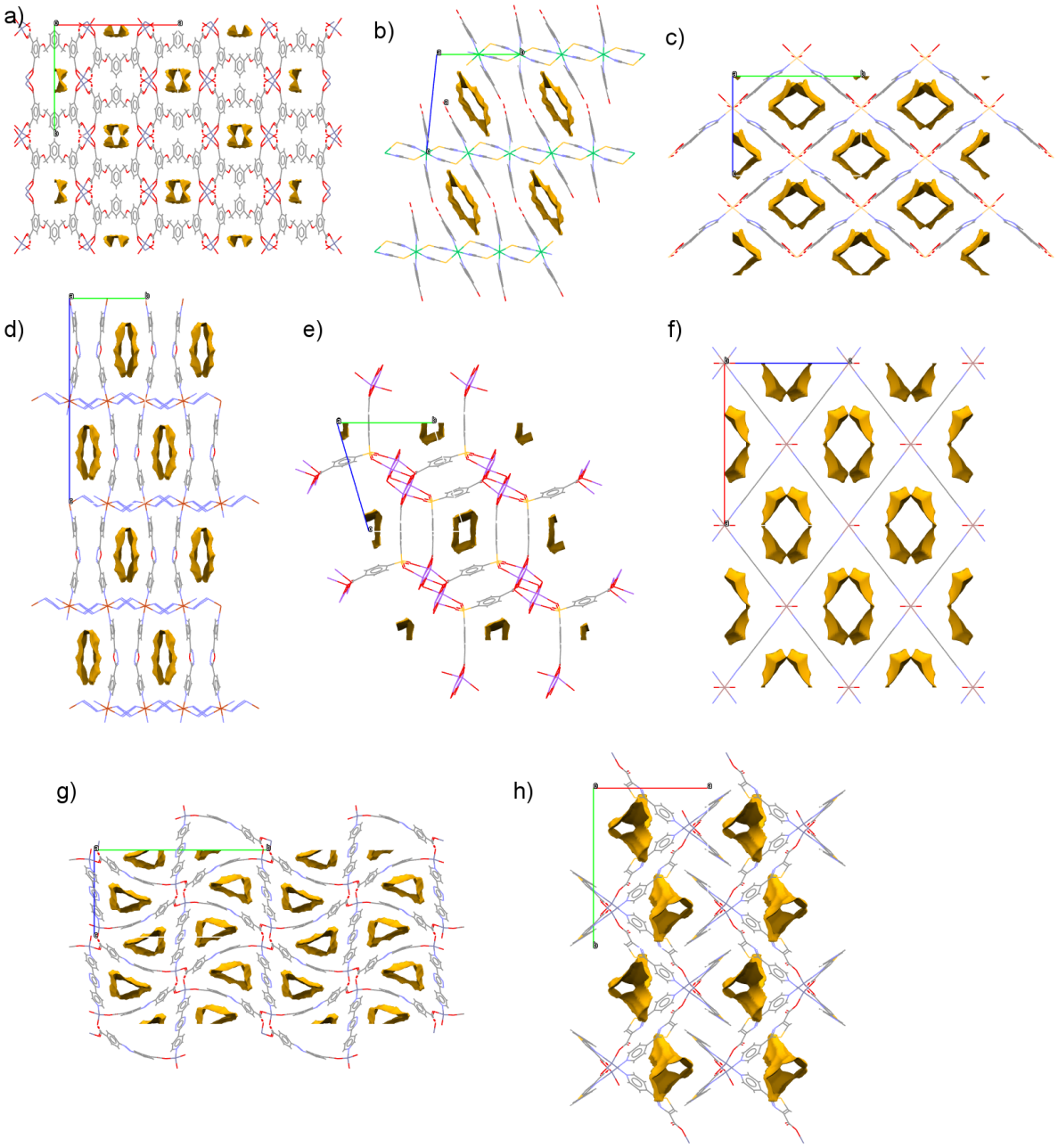

Figure S7. *Snapshots of the void space in the top structures - QOKCID (a), FARZEE (b), RUVBER (c), ISAYUW (d), HISFUM (e), SOMSIY (f), KURSOH (g), LENROM (h). Reference codes taken from the Cambridge Structural Database.*[14]

References

1. A. K. Rappe, C. J. Casewit, K. S. Colwell, W. A. Goddard and W. M. Skiff, *J. Am. Chem. Soc.*, 1992, **114**, 10024-10035.

2. M. G. Martin and J. I. Siepmann, *J. Phys. Chem. B.*, 1998, **102**, 2569-2577.

3. J. J. Potoff and J. I. Siepmann, *AIChE J.*, 2001, **47**, 1676-1682.

4. T. Kristóf and J. Liszi, *J. Phys. Chem. B.*, 1997, **101**, 5480-5483.

5. H. W. Horn, W. C. Swope, J. W. Pitera, J. D. Madura, T. J. Dick, G. L. Hura and T. Head-Gordon, *J. Chem. Phys.*, 2004, **120**, 9665-9678.

6. Y. Liu, Z. Ng, E. A. Khan, H. K. Jeong, C. b. Ching and Z. Lai, *Microporous Mesoporous Mater.*, 2009, **118**, 296-301.

7. D.-J. Lee, Q. Li, H. Kim and K. Lee, *Microporous Mesoporous Mater.*, 2012, **163**, 169-177.

8. S. R. Venna and M. A. Carreon, *J. Am. Chem. Soc.*, 2010, **132**, 76-78.

9. A. Huang, W. Dou and J. Caro, *J. Am. Chem. Soc.*, 2010, **132**, 15562-15564.

10. J. A. Bohrman and M. A. Carreon, *Chem. Commun. (Cambridge, U. K.)*, 2012, **48**, 5130-5132.

11. T. F. Willems, C. H. Rycroft, M. Kazi, J. C. Meza and M. Haranczyk, *Microporous Mesoporous Mater.*, 2012, **149**, 134-141.

12. D. Ongari, P. G. Boyd, O. Kadioglu, A. K. Mace, S. Keskin and B. Smit, *J. Chem. Theory Comput.*, 2019, **15**, 382-401.

13. C. F. Macrae, I. Sovago, S. J. Cottrell, P. T. A. Galek, P. McCabe, E. Pidcock, M. Platings, G. P. Shields, J. S. Stevens, M. Towler and P. A. Wood, *J. Appl. Cryst.*, **53**, 226-235, 2020

14. The Cambridge Structural Database, https://www.ccdc.cam.ac.uk/structures/, (*accessed November 2020*)